A Preliminary Structural Analysis of Space-Based Inflatable Tubular Frame Structures

J. A. Main S. W. Peterson A. M. Strauss

Dept. of Mechanical Engineering
Vanderbilt University
Box 1592, Station B
Nashville, TN 37235 USA

ABSTRACT

The use of inflatable structures has often been proposed for aerospace and planetary applications. The advantages of such structures include low launch weight and easy assembly. This paper proposes the use of inflatables for applications requiring very large frame structures intended for aerospace use.

In order to consider using an inflated truss the structural behavior of the inflated frame must be examined. The statics of inflated tubes as beams has been discussed in the literature, but the dynamics of these elements has not received much attention. In an effort to evaluate the vibration characteristics of the inflated beam a series of free vibration tests of an inflated fabric cantilever were performed. Results of the tests are presented in this paper and models for system behavior posed.

NOMENCLATURE

a_n	constant in natural frequency calculation
l	inflated beam length (m)
p	beam inflation pressure (Pa)
r	radius of inflated beam (m)
t	time (s)
x	beam coordinate from beam tip (m)
y	beam deflection (m)
E	beam fabric modulus (N/m)
I	inflated beam moment of inertia (m^3)
Kin	kinetic energy (joules)
M	applied bending moment (N-m)
N	axial stress resultant (N/m)
Pot	potential energy (joules)
V_1	volume of beam when undeflected (m^3)
V_2	volume of beam at maximum deflection (m^3)
μ	beam mass per unit length (kg/m)
ρ	radius of curvature (m)
θ	angular position (radians)
ω	angular frequency (radians/s)

INTRODUCTION

Interest in using inflatable structures in space exists because their basic characteristics (Leonard, 1974) solve many engineering problems that the structural designer is faced with in space. Pneumatic structures consist of no more than a few layers of fabric and can be launched into space in their uninflated state, so the launch penalty associated with them is very low. Also, they can be prefabricated, packed, and then deployed in space by pressurization. There are questions, however, about the safety and durability of inflated structures in the space environment.

The initial space-based application of inflated structures, also called pneumatic structures, was ECHO-1, launched in August of 1960. ECHO-1 was a 30 m diameter metallized mylar balloon that was used as a passive telecommunications satellite. Similar pneumatic structures were sent aloft as ECHO-2 in 1964 and PAGEOS-1 in 1966.

Examples of more complex space-based inflated structures that go a step beyond the simple spherical balloons used in ECHO and PAGEOS were designed and tested by the Goodyear Aerospace Corporation under contract from NASA during the Apollo and Skylab programs in the 1960's and 70's. These included the Lunar Stay Time Extension Module (Tynan, 1965), MOBY DICK (French, 1967), and the D021 airlock (Manning and Jurich, 1973).

Numerous proposals have also been made to use more complex inflatables for large space structures such as precision antenna reflectors (Girard et al., 1982; Reibaldi, 1985; Authier and Hill, 1985; Bernasconi and Reibaldi, 1986; Williams, 1988), solar concentrators (Mikulas and Hedgepeth, 1989; Grossman and Williams, 1989), orbiting hangars (Ohkami et al., 1986), and inflatable construction forms (Kaden and Pense, 1988). It has also been suggested that inflatable segments be used to replace the solid portions of the space shuttle robot arm to reduce arm inertia and minimize required storage space (McCarty, 1990).

In 1962 Frei Otto's Tensile Structures was first published, a work that was largely devoted to outlining numerous past, present and future applications of pneumatic structures. Otto presents scores of intriguing ideas for novel applications of pneumatic structures. Of particular interest to this investigation are the concepts that use inflated cylindrical beams as structural members. The choice of the inflated cylinder as structural member is natural: a piece of fabric sewn into a closed tube will assume the shape of a cylinder when internally

pressurized. The ease of fabrication and ability to span distances and carry loads make the inflated cylinder the natural pneumatic analog to the elastic beam. Reenforcing this analogy are Otto's conceptual designs that include inflated cylindrical beams as members in planar and space trusses.

Current strategies for open frame structures intended for aerospace use include both deployable and erectable structures. Deployable trusses are those that are folded or packed and then remotely expanded upon reaching orbit. Erectable trusses use standardized beam elements that connect into a node fixture. The strength and reliability of the solid members of these truss designs make them the practical choice for the truss component in current space station designs. However, when future needs require construction of extremely large truss structures, perhaps with dimensions measured in kilometers rather than meters, the amount of material to be lifted and the extravehicular activity required for construction of solid element trusses may become prohibitive. The advantages of inflatables may outweigh their shortcomings in these applications.

ANALYSIS OF THE INFLATED BEAM: STATICS

If the inflatable truss structure concept is to be successfully implemented structural models must be developed to predict both their static and dynamic behavior in the space environment. Structural analysis of inflated circular-cylindrical beams has been performed using a number of different strategies. Linear shell analyses have been used to model the buckling behavior and shear deflections(Leonard et al., 1960; Topping, 1964; Bulson, 1973) of inflated members. Stiffness of inflated cantilever beams has also been modelled with nonlinear methods (Douglas, 1969) and variational methods have been used with shell models of inflated beams to determine beam deflections under a variety of loads (Steeves, 1975). Comer and Levy (1963) modelled the behavior of an inflated cantilever beam in a manner similar to conventional beam theory. The following deflection analysis of the inflated beam closely follows the method used by Comer and Levy with some modifications to make the results more applicable to fabric structures. These changes include the use of stress resultants instead of stress and expressing fabric modulus in terms of force per unit width. This was done because fabric thickness can only be vaguely correlated with load carrying ability.

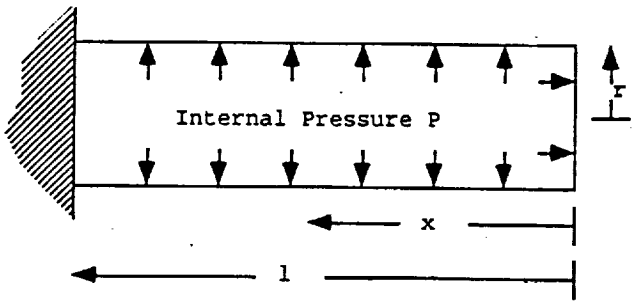

Figure 1. Sketch of the inflated cantilever.

Figure 1 shows a sketch of an inflated cantilever beam. An arbitrary loading of this beam can be expressed as applied moments that are a function of the beam coordinate x. A model of an inflated structure must accommodate both slack and taut regions in the fabric. In the taut regions, or when the axial stress in a given cross-section of the fabric of an inflated beam remains tensile around the complete circumference, the stress distribution illustrated in Figure 2 is assumed.

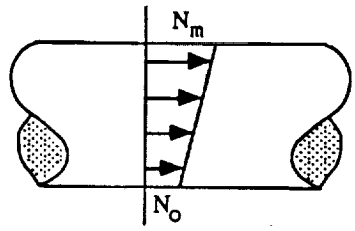

Figure 2. The stress distribution in the fabric of the inflated beam in regions where no wrinkling is present.

In these regions the value of the axial stress resultant in the beam skin is defined as

$$N = N_o \left(\frac{1 + \cos\theta}{2}\right) + N_m \left(\frac{1 - \cos\theta}{2}\right) \qquad (1)$$

In this expression θ is measured around the circumference of the beam from the point where $N = N_o$.

When the applied moment exceeds the value $\pi r^3 p/2$ the bending stress cancels the axial stress in the fabric skin on the concave side of the beam and wrinkling will begin in that region. The fabric wrinkles because it is incapable of resisting compressive loads. In these regions the stress distribution illustrated in Figure 3 is assumed.

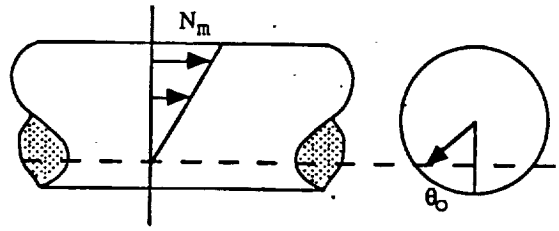

Figure 3. The stress distribution in the fabric of the inflated beam in regions where wrinkling occurs.

In these regions the stress resultant in the axial direction is the fabric skin is

$$N = \left(\frac{\cos\theta_o - \cos\theta}{1 + \cos\theta_o}\right) N_m \qquad \pi > \theta > \theta_o$$

$$N = 0 \qquad \theta_o > \theta > 0 \qquad (2)$$

For the balance of moments about a transverse axis through the center of the beam a distance x from the tip

$$M(x) = -2 \int_0^{\pi} N\, r^2 \cos\theta \, d\theta \qquad (3)$$

When $M > \pi r^3 p/2$ equations 2 and 3 can be combined to give

$$N_m = \frac{2\,M(x)\,(1+\cos\theta_o)}{r^2\,(2\pi - 2\theta_o + \sin 2\theta_o)} \qquad (4)$$

For a balance of axial forces on the endplate

$$p\pi r^2 = 2\int_0^{\pi} N\,r\,d\theta \qquad (5)$$

Again considering the regions containing wrinkled fabric, equations 2 and 5 can be combined to give

$$N_m = \frac{p\pi r\,(1+\cos\theta_o)}{2\,((\pi-\theta_o)\cos\theta_o + \sin\theta_o)} \qquad (6)$$

Equating the expressions for Nm in equations 4 and 6 yields

$$\frac{M(x)}{pr^3} = \frac{\pi\,(2\pi - 2\theta_o + \sin 2\theta_o)}{4\,((\pi-\theta_o)\cos\theta_o + \sin\theta_o)} \qquad (7)$$

Considering now the regions where no wrinkling of the cross section occurs, substitution of equation 1 into equation 3 gives

$$N_m - N_o = 2\,M(x)/\pi r^2 \qquad (8)$$

Substituting equation 1 into equation 5 yields

$$N_m + N_o = pr \qquad (9)$$

Combining equations 8 and 9 yields

$$N_m = (M(x)/\pi r^2) + (pr/2) \qquad (10)$$

The curvature of a beam element that is part of a wrinkled region is given by

$$\frac{1}{\rho} = \frac{(N_m/E)}{r(1+\cos\theta_o)} \qquad (11)$$

Substituting in the expression for N_m in equation 4 yields

$$\frac{1}{\rho} = \frac{2\,M(x)}{E\,r^3(2\pi - 2\theta_o + \sin 2\theta_o)} \qquad (12)$$

The curvature of elements in the unwrinkled regions is given by

$$\frac{1}{\rho} = \frac{(N_m - N_o)}{2\,E\,r} \qquad (13)$$

Substituting equation 8 into equation 13 yields

$$\frac{1}{\rho} = \frac{M(x)}{\pi\,r^3\,E} \qquad (14)$$

Equations 12 and 14 can be combined and the approximation $1/\rho = d^2y/dx^2$ applied so that the entire system of equations can be expressed in the following form:

$$\frac{d^2y}{dx^2} = \frac{M(x)}{E\,I} \qquad (15)$$

$$I = r^3\,(\pi - \theta_o + (\sin 2\theta_o)/2) \quad \text{for } M > \pi p r^3/2$$

$$I = \pi\,r^3 \quad \text{for } M < \pi p r^3/2$$

For the regions of the beam that are wrinkled ($M > \pi r^3 p/2$) equation 7 must be used to determine the angle θ_o that corresponds with the applied moment. Beam deflections can be obtained by numerically solving the differential equation of bending.

ANALYSIS OF THE INFLATED BEAM: DYNAMICS

Dynamic modelling methods that have been applied to inflated beams include spring-inertia models and simple potential energy models (Main et al., 1991). Accurate dynamic models of space-based structures are important because unexpected vibration problems have been encountered in orbiting structures that have compromised the sensitivity of the instruments they carry, and unexpected dynamic effects could also compromise structural integrity.

In the previous section an analysis method for the inflated cantilever was outlined that is analogous to the shear-moment method of elastic beam analysis. Expanding on this analogy, Leonard (1988) suggested that elastic beam flexural modes be used to approximate the lower natural frequencies of an inflated beam. The expression for the natural frequency of the nth mode of vibration of a solid elastic cantilever beam is

$$\omega_n = a_n\sqrt{(E\,I)/(\mu\,l^4)} \qquad (16)$$

The constant a_n equals 3.52 and 22.0 for the first and second modes, respectively (Den Hartog, 1985).

Despite the similarities between the two systems, there are important characteristics that distinguish the inflated beam from the elastic beam. In particular, the effects of the change in volume and the associated change in pressure of the the enclosed gas of the beam should be examined as the physical cause of a natural oscillation of the inflated cantilever.

One method of determining the frequency of vibration of a dynamic system is to consider the balance between the kinetic and potential energies. In the inflated beam the pressurization medium is compressed and expands as the enclosed volume changes during each cycle, thus changing the potential energy of the system.

To determine the potential energy stored as the volume of the beam changes during each cycle the undeformed and deformed volumes of the beam must be calculated. Consider the element of the inflated beam sketched in Figure 4.

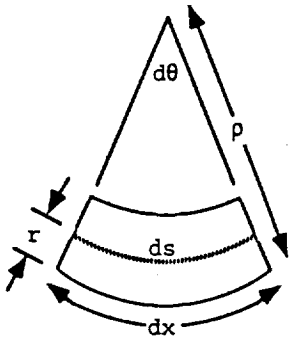

Figure 4. An element of an inflated beam.

The undeformed volume of this element is

$$dV_1 = \pi r^2 \, dx \tag{17}$$

The deformed volume of the beam can be approximated by assuming the beam fabric to be inextensible. The length of the centerline is then related to the element length as follows.

$$dx - ds = r \, d\theta \tag{18}$$

Multiplying through by the cross-sectional area of the beam allows the volume difference between the undeformed and deformed element to be determined.

$$dV_1 - dV_2 = \pi r^3 \, d\theta \tag{19}$$

From the geometry of the deformed element we have $d\theta = dx/\rho$. Further incorporating this and the approximation $1/\rho = d^2y/dx^2$ into equation 19 yields

$$dV_1 - dV_2 = \pi r^3 \left(\frac{d^2y}{dx^2}\right) dx \tag{20}$$

Combining this result with equation 17 and integrating yields expressions for both the undeformed and deformed volumes of the beam.

$$V_1 = \pi r^2 l$$
$$V_2 = \pi r^2 l - \int_0^l \pi r^3 \left(\frac{d^2y}{dx^2}\right) dx \tag{21}$$

If we assume the process of compression and expansion of the gas in the beam to be quasi-static, the potential energy stored in the gas during each compression cycle is

$$Pot = -p_1 V_1 \ln\left(\frac{V_2}{V_1}\right) \tag{22}$$

The total kinetic energy of the inflated fabric cantilever in free vibration is the sum of the kinetic energies of each element dx.

$$dKin = \frac{1}{2} (\mu \, dx) (y\omega)^2 \tag{23}$$

This expression assumes that each point on the beam vibrates such that

$$y(x,t) = y_o(x) \sin\omega t \tag{24}$$

The expression for the total kinetic energy of the beam is therefore

$$Kin = \frac{1}{2} \mu\omega^2 \int_0^l y^2 \, dx \tag{25}$$

Equating the expressions for the beam potential and kinetic energies yields the following expression for beam natural frequency.

$$\omega^2 = \frac{-2 \, p_1 V_1 \ln\left(\frac{V_2}{V_1}\right)}{\mu \int_0^l y^2 \, dx} \tag{26}$$

To solve this equation for a particular vibration amplitude the uniform inertial load level necessary for deflecting the beam the desired amount must be determined. This is done by iteratively solving equations 15 and 7 for a range of uniform loads until the load that results in the desired tip deflection is determined. Once this load level is determined and the numerical solution to the beam deflection differential equation has been obtained, the results can be substituted into equation 26 and the frequency of vibration due to the expansion and compression of the gas determined. Vibration frequencies for a range of amplitudes can be obtained by repeating this procedure over a range of load levels.

EXPERIMENTAL

An inflated cylindrical cantilever beam was constructed by combining an outer rip-stop nylon restraint layer with an internal gastight vinyl bladder. (See Figure 5) The resulting structure had a length of 1.0605 m and was 0.0928 m in diameter. The base of the cantilever was solidly mounted to a large building column and a free vibration test was performed. Slight beam curvature was noted due to gravity resulting in a downward tip deflection of approximately 2 cm. The beam vibration was initiated by horizontally displacing the tip of the cantilever approximately 5 cm and then releasing it. This initial deflection was chosen with reference to the results of the previous investigators to be well short of the level that would cause beam buckling. A free vibration spectrum was obtained by mounting a Bruel and Kjear Model 4366 accelerometer on the tip of the beam. All tests were performed with the beam pressurized to 69 kPa (10 PSI).

NUMERICAL AND EXPERIMENTAL RESULTS

The expression for beam natural frequency in equation 16 was used to determine the lower natural frequencies of the inflated beam. Tensile tests on the beam restraint fabric demonstrated that it had a modulus of approximately 30,000 N/m. The masses of the fabric restraint, vinyl bladder, and the enclosed nitrogen gas combined to give a beam mass per unit length of 0.092 kg/m. With these results the first and second modes of vibration were calculated to be 4.60 and 28.76 Hz, respectively.

The frequency of vibration due to the projected change in the volume of the beam was calculated from equation 26. The beam curvatures and displacements were calculated from equation 15 by assuming that the beam is subject to a uniform load of a magnitude necessary for a given tip deflection. Since the displacements and curvatures of the beam are dependent upon the magnitude of the applied uniform load, the vibration frequency calculated from those parameters is amplitude dependent. The differential equation solver DASSL was used to find the curvatures and displacements along the length of the beam for each incremental load level. Solutions were generated for a range of amplitudes up to the 5 cm maximum amplitude.

The resulting amplitude vs. frequency plot and the two lowest natural frequencies of the beam are shown in Figure 6. The curves are truncated at the 5 cm amplitude level to correspond with the initial tip deflection of the beam during the free vibration tests. The predicted frequency of vibration of 4.60 Hz is easily identifiable in the experimental spectrum. The second mode, at 28.76 Hz, is less evident. The peak from 40 to 57 Hz seems to correspond well with the gas compression/expansion model curve in the 1 to 3 cm amplitude range.

SUMMARY

Comparison of the model results with the experimentally obtained free vibration spectrum of the inflated cantilever indicate that accurate predictions of the frequencies of vibration for the lower modes can indeed be made using conventional beam flexural modes. There does exist approximately a 16% discrepancy between the calculated and measured frequency of the first mode. Considering the complexity of the system and the assumptions necessary for development of the model it is the opinion of the authors that this difference is not unreasonable.

The correspondence between the gas compression/expansion model and the experimental data is encouraging, but not yet conclusive as to whether or not the corresponding peak in the experimental spectrum is due to this physical process. A definitive answer to this question might be obtained by repeating the free vibration test and simultaneously recording the pressure variations inside the beam.

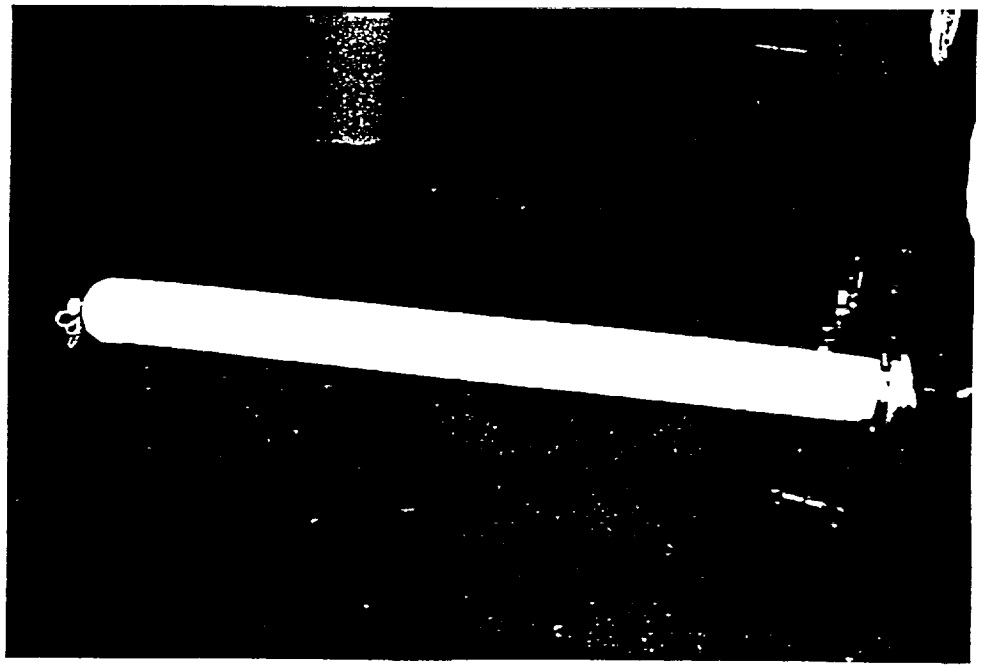

Figure 5. Photo of inflated cantilever test assembly.

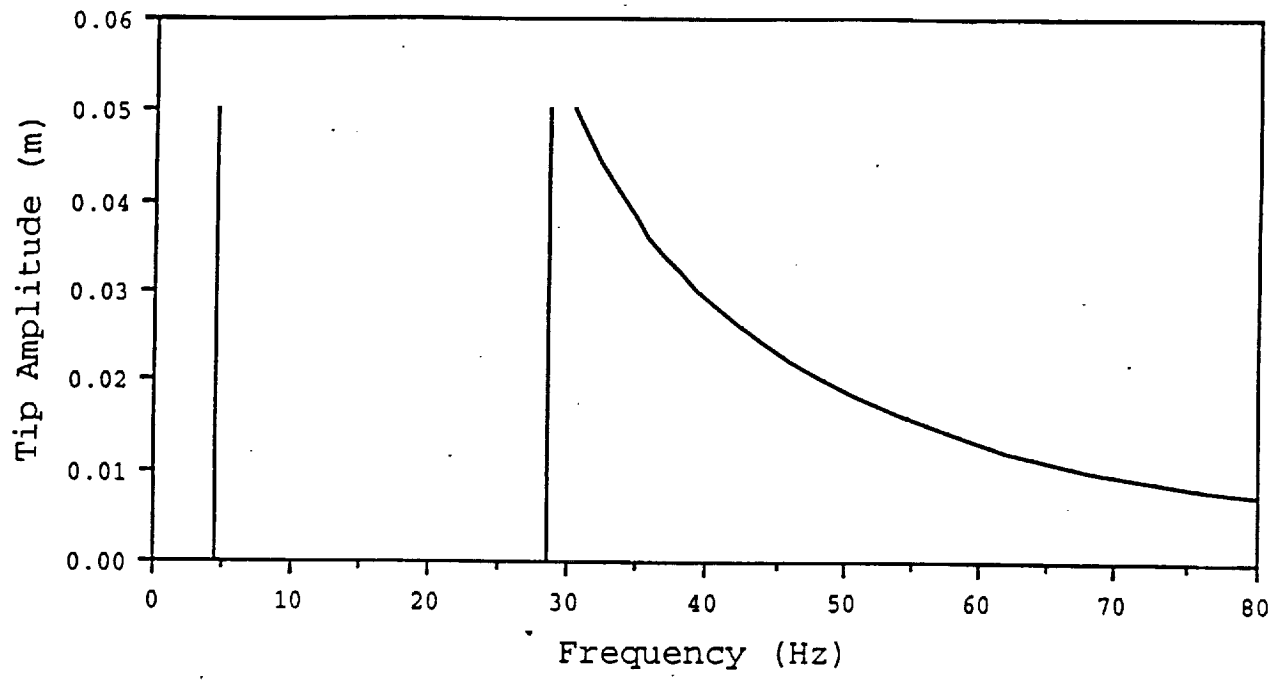

Figure 6. Plot showing the calculated frequencies of vibration of the inflated cantilever. The two spikes on the left are first and second modes of vibration according to beam theory. The curve on the right shows the amplitude dependent vibration frequencies of the beam from the gas compression/expansion model.

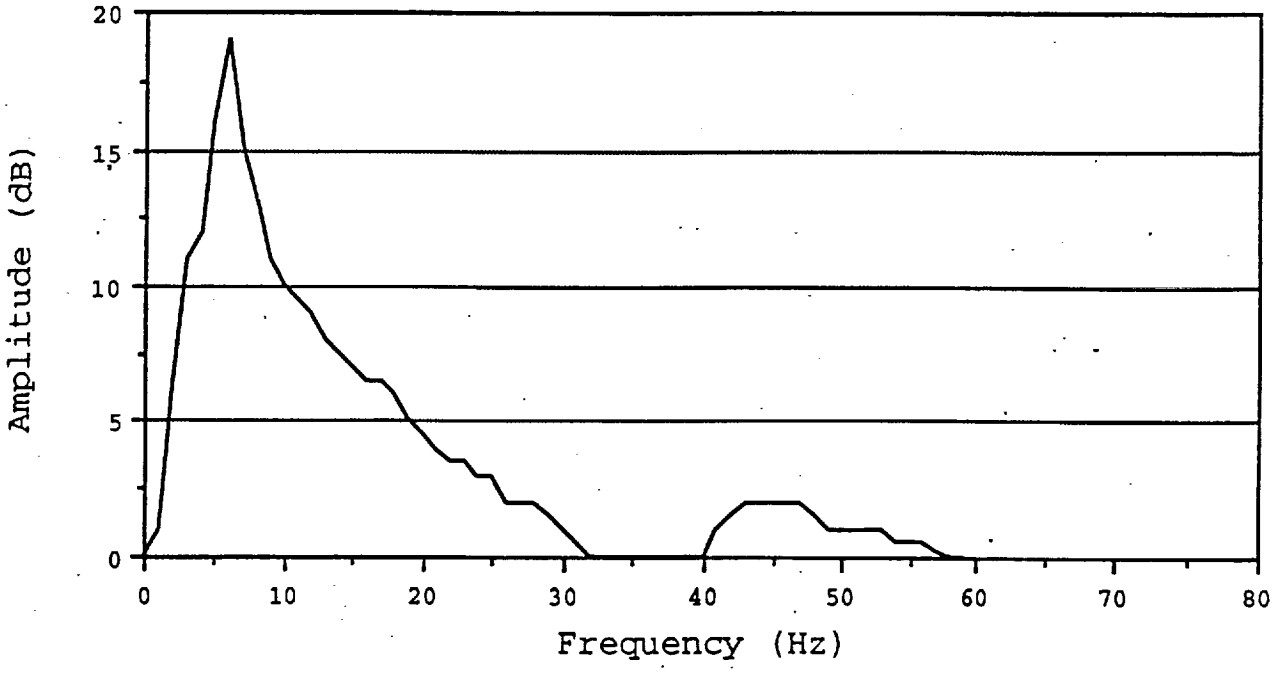

Figure 7. Experimentally obtained free vibration spectrum of the inflated cantilever test specimen. The initial tip amplitude of the beam was 5 cm.

ACKNOWLEDGEMENTS

The authors would like to thank the NASA Office of Aeronautics and Exploration Technology and the NASA National Space Grant College and Fellowship Program.

REFERENCES

Authier, B., and Hill, L., "Large Inflatable Parabolic Reflectors in Space," Instrumentation for Submillimeter Spectroscopy 598 (1985): 126-132.

Bernasconi, M. C. , and Reibaldi, G. G., "Inflatable, Space-Rigidized Structures: Overview of Applications and Their Technology Impact," Acta Astronautica 14 (1986): 455-465.

Bulson, P. S., "Design Principles of Pneumatic Structures," The Structural Engineer 51 (June 1973): 209-215.

Comer, R. L., and Levy, S., "Deflections of an Inflated Circular-Cylindrical Cantilever Beam," AIAA Journal 1 (July 1963):1652-1655.

Den Hartog, J. P., Mechanical Vibrations (Mineola NY, Dover, 1985), 141-147.

Douglas, W. J. "Bending Stiffness of an Inflated Cylindrical Cantilever Beam," AIAA Journal 7 (July 1969): 1248-1253.

French, R. J., A Feasibility Investigation of Expandable Structures Module for Orbital Experiment - Artificial G, (Goodyear Aerospace Report under NASA contract), NTIS, N67-30000.

Girard, L., Bloetscher, F., and Stimler, F., Innovative Structures for Space Applications, (Goodyear Aerospace Report GAC 19-1563, October 1982), NTIS, N84-25757.

Grossman, G., and Williams, G., "Inflatable Concentrators for Solar Propulsion and Dynamic Space Power," in Solar Engineering - 1989, Proceedings of the Eleventh Annual ASME Solar Energy Conference held in San Diego, CA, April, 1989.

Kaden, R. A., and Pense, L. D., "Planetary Base Inflatable Form Construction," in Engineering, Construction, and Operations in Space, Proceedings of Space 88 held in Albuquerque, NM, August 1988.

Leonard, J. W., "State-of-the-Art in Inflatable Shell Research," ASCE Journal of the Engineering Mechanics Division 1 (February 1974): 17-25.

Leonard, J. W., Tension Structures (New York NY, McGraw-Hill, 1988), 246-247.

Leonard, R. W., Brooks, G. W., and McComb, H. G. Jr., Structural Considerations of Inflatable Reentry Vehicles (NASA Technical Note D-457, September 1960).

McCarty, L. H., "Inflatable Arm Segments May Lighten Shuttle's Manipulator System," Design News (April 9, 1990): 150-151.

Main, J. A., Peterson, S. W., Strauss, A. M., "Design of Space-Based Inflatable Tubular Frame Structures," in Paper Presented at the International Design for Extreme Environments Assembly in Houston, TX in November 1991.

Manning, L., and Jurich, L., Expandable Airlock Experiment (DO21) and the Skylab Mission, (Goodyear Aerospace Report under U. S. Air Force contract, September 1972), NTIS, N73-15896.

Mikulas, M. M., and Hedgepeth, J. M., "Structural Concepts for Very Large (400-Meter-Diameter) Solar Concentrators," in Second Beamed Space-Power Workshop, Proceedings of a NASA workshop at Langley Research Center, Hampton, VA, February 1989, NTIS, N90-10153.

Ohkami, Y., Matsumoto, K., Kida, T., IIda, T., and Sakai, J., "An Enclosed Hangar Concept for Large Spacecraft Servicing at Space Station," in Proceedings: 15th International Symposium on Space Technology and Science held in Tokyo, Japan, May 1986.

Otto, F., Tensile Structures (Cambridge MA, MIT Press, 1962), 86-87.

Reibaldi, G. G., "Inflatable Technology in Orbit Demonstration Within the European Space Agency Programs," in 25th International Conference on Space held in Rome, Italy, March 1985.

Steeves, E. C., A Linear Analysis of the Deformation of Pressure Stabilized Tubes (U. S. Army Natick Laboratories report, AD/A-006 493, January 1975), NTIS, N75-32513.

Topping, A. D., "Shear Deflections and Buckling Characteristics of Inflated Members," Journal of Aircraft 1 (Sept.-Oct. 1964): 289-293.

Tynan, C. W. Jr., "Lunar Stay Time Extension Module," in Selected Papers on Environmental and Attitude Control of Manned Spacecraft, (NASA, June 1965), NTIS, N67-14250.

Williams, G., "Inflatable Antennas for Microwave Power Transmission," in Free-Space Power Transmission, Proceedings of a NASA workshop at Lewis Research Center, Cleveland, Ohio, March 1988, NTIS, N90-21799.